Journal Name

ROYAL SOCIETY OF CHEMISTRY

ARTICLE TYPE

Cite this: DOI: 10.1039/xxxxxxxxxx

Interactions between a water molecule and C_{60} in the endohedral fullerene $H_2O@C_{60}$†

Effat Rashed,[a] and Janette L Dunn*[a]

Received Date
Accepted Date

DOI: 10.1039/xxxxxxxxxx

www.rsc.org/journalname

A water molecule encapsulated inside a C_{60} fullerene cage behaves almost like an asymmetric top rotor, as would be expected of an isolated water molecule. However, inelastic neutron scattering (INS) experiments show evidence of interactions between the water molecule and its environment [Goh *et al., Phys. Chem. Chem. Phys.*, 2014, **16**, 21330]. In particular, a resolved splitting of the 1_{01} rotational level into a singlet and a doublet indicates that the water molecule experiences an environment of lower symmetry than the icosahedral symmetry of a C_{60} cage. Recent calculations have shown that the splitting can be explained in terms of electrostatic quadrupolar interactions between the water molecule and the electron clouds of nearest-neighbour C_{60} molecules, which results in an effective environment of S_6 symmetry [Felker *et al.*, *Phys. Chem. Chem. Phys.*, 2017, **19**, 31274 and Bačić *et al.*, *Faraday Discussions*, 2018, doi:10.1039/C8FD00082D]. We use symmetry arguments to obtain a simple algebraic expression, expressed in terms of a linear combination of products of translational and rotational basis functions, that describes the effect on a water molecule of any potential of S_6 symmetry. We show that we can reproduce the results of the electrostatic interaction model up to ≈ 12 meV in terms of two unknown parameters only. The resulting potential is in a form that can readily be used in future calculations, without needing to use density functional theory (DFT) for example. Adjusting parameters in our potential would help identify whether other symmetry-lowering interactions are also present if experimental results that resolve splittings in higher-energy rotational levels are obtained in the future. As another application of our model, we show that the results of DFT calculations of the variation in energy as a water molecule moves inside the cage of an isolated C_{60} molecule, where the water molecule experiences an environment of icosahedral symmetry, can also be reproduced using our model.

1 Introduction

In 2011, the endohedral $H_2O@C_{60}$ fullerene was first synthesized, using a process known as molecular surgery.[1] The relatively large inner cavity of C_{60} together with the absence of strong interactions between the water molecule and the C_{60} molecule provides a highly symmetric, nano-size laboratory in which the single-molecule behaviour of the encapsulated water molecule can be explored. ^{13}C NMR and and ultraviolet-visible (UV-Vis) spectroscopy indicate that an encapsulated water molecule will rotate rapidly, at least on the timescale of NMR.[1] Nuclear spin conversion in NMR also shows that the rotation is almost free,[2] as do Molecular Dynamics (MD) simulations.[3] This confirms that any interactions that do exist between the water molecule and the C_{60} cage must be weak. However, non-covalent interactions resulting from the interplay between van der Waals (vdW) and hydrogen-bonding interactions[4] still have measurable effects on the properties of the water molecule.

Intermolecular interactions also affect the structural properties of solid $H_2O@C_{60}$. X-ray diffraction experiments indicate that the structure of crystalline $H_2O@C_{60}$ is very similar to that of empty C_{60} solids. At temperatures below 90 K, it has a simple cubic structure (of space group $Pa\bar{3}$).[5] The individual C_{60} molecules are locked in one of two standard orientations,[6–8] in a ratio of 5:1. In the dominant orientation, known as the P orientation, the double bond joining two hexagons on one molecule faces the centre of a pentagon on a neighbouring molecule. In the other orientation, known as the H orientation, the double bond faces a hexagon.[8]

Calculations have shown that the symmetry of the minimum-energy configuration of an isolated $H_2O@C_{60}$ molecule is C_2,[4,5] although the orientation of the water molecule is such that the symmetry is nearly C_{2v},[5] and the energy of the fully-C_{2v} configuration is only slightly higher.[4] In both C_2 and C_{2v} symmetries, the dipole axis of the water molecule points towards the centre

[a] *School of Physics & Astronomy, University Park, Nottingham, UK. Fax: +44 115 9515180; Tel: +44 115 9515135; E-mail: janette.dunn@nottingham.ac.uk*

† Electronic Supplementary Information (ESI) available: [details of any supplementary information available should be included here]. See DOI: 10.1039/b000000x/

of the C_{60} cage. However, as the C_{60} molecule contains ten C_2 axes, there are multiple equivalent minimum-energy configurations. The water molecule will undergo a (hindered) rotation between these configurations. The timescale of the interconversion is rapid, so the water molecule appears to be rotating in experimental measurements. As the water molecule moves between equivalent configurations, there is both a rotation about its centre of mass and a translation of its centre of mass. The translational and rotational motions are both quantised, and the coupled translational and rotational motion can be described by symmetry-adapted states that inherently embody translation-rotation (TR) coupling. These states will reflect the symmetry of the environment in which the water molecule moves, which will be higher than the symmetry (C_2 or C_{2v}) of the minimum-energy configurations of an isolated $H_2O@C_{60}$ molecule. The situation is analogous to the dynamic Jahn-Teller (JT) effect in an empty C_{60} ion, where coupling between the electrons and the vibrational motion of the carbon nuclei results in an instantaneous distortion of the fullerene cage but tunnelling between equivalent minimum-energy configurations results in symmetry-adapted states that have the same icosahedral symmetry as the undistorted ion.[9]

H_2O is an asymmetric top rotor, whose rotational energy levels can be classified using (integer) quantum numbers $J_{k_a k_c}$, where $J = 0, 1, 2, ...$ is the total angular momentum. k_a and k_c relate to angular momentum about the molecule-fixed principal axes a with the smallest moment of inertia and c with the largest moment of inertia respectively. Hence both k_a and k_c lie in the range $-J$ to $+J$. They are exact quantum numbers in the prolate and oblate top limits respectively.[10] The $J_{k_a k_c}$ states have a degeneracy of up to $(2J+1)$, so they can be split under the influence of symmetry-lowering interactions. The states can be further classified into *para-* (total nuclear spin $I = 0$) and *ortho-* ($I = 1$) states. The Pauli exclusion principle requires that *para-* states correlate with even $k_a + k_c$ and *ortho-* states with odd $k_a + k_c$. The ground state of *para*-water is a singlet 0_{00} and the ground state of *ortho*-water is the triplet state 1_{01}.

Recent inelastic neutron scattering (INS) experiments have revealed the existence of a small splitting in the 1_{01} state into a lower lying singlet 1^a_{01} at 2.61 meV and an upper lying doublet 1^b_{01} at 3.09 meV relative to the *para*-ground state 0_{00},[11] with a further small shoulder on the side of the 2.61 meV peak at around 2.46 meV.[12] The fine structure of levels higher than 1_{01} was not resolved in the INS spectra. The splitting of the 1_{01} level into a singlet and doublet indicates that the water molecule must be subject to an environment with a symmetry lower than icosahedral; I_h symmetry does not support doublet representations, so cannot be responsible for a splitting of the 1_{01} triplet into a singlet and a doublet (and, as can be shown using symmetry arguments, can't split 1_{01} into three singlets with an accidental degeneracy).

Observed energy level splittings in $H_2O@C_{60}$, as well as in $H_2@C_{60}$ and $HF@C_{60}$ have all recently been analysed using a model involving electrostatic quadrupole interactions between the charge densities on an encapsulated water molecule and on neighbouring C_{60} cages.[13,14] This model took a filled C_{60} molecule to be surrounded by 12 empty molecules in either the P or the H orientation, with all of the C_{60} cages retaining their icosahedral symmetry. The cluster analysed has S_6 symmetry,[15] which is consistent with the simple cubic ($Pa\bar{3}$) structure of a C_{60} solid at low temperatures and does support singlet and doublet representations. The model provides a good match to the split 1_{01} levels. Splittings in higher excited states can't currently be resolved experimentally. Therefore it is difficult to assess how well the results of the electrostatic interaction model match the energies of the excited states. It was originally suggested that the reduction in the symmetry of the environment seen by an encapsulated water molecule could be due to intramolecular JT or JT-like interactions causing a distortion of the C_{60} cage.[11,12] Crystal field effects could also be operating. Further experiments are needed to determine whether there is evidence for any additional symmetry-lowering interactions, or whether electrostatic interactions are the only significant symmetry-lowering interaction.

In this paper, we will use symmetry arguments to construct a potential of S_6 symmetry from an expansion in terms of translational and rotational states of the water molecule. In this way, it doesn't matter what causes the reduction in symmetry.[16] We will discuss how our results compare to those of the electrostatic interaction model for a certain choice of parameters, and how choosing different parameters will account for the presence of additional interactions. This will be important if experimental results that resolve splittings in higher excited states become available in the future. Also, as our potential has a simple analytical form, it is easy to incorporate it in future calculations without the need to carry out computationally-expensive DFT calculations for example. As a further example of how our model can be applied, we will construct an equivalent potential of icosahedral (I_h) symmetry, and show that it can be used to reproduce the results of DFT calculations showing the variation in energy of a water molecule as it moves along certain radial directions inside the cage of an isolated C_{60} molecule.

We will start by constructing states of both S_6 and I_h symmetries from linear combinations of products of rotational and translational states of the water molecule. These states inherently incorporate TR coupling, so there is no advantage in using a basis that couples rotational and translational angular momentum as in the work of Felker and Bačić.[17] Our states are also automatically either symmetric or antisymmetric under an exchange of the two H atoms. The group combining I_h with permutations of the H atoms, i.e. the group which is a direct product of I_h and the full permutation group S_2, has been called $I_h^{(12)}$. Its states have been labelled according to irreducible representations (irreps.) $\Gamma^{(s)}$ and $\Gamma^{(a)}$ to indicate whether they are symmetric (invariant) or antisymmetric (change sign) respectively under exchange of the two H atoms.[17] This group was originally developed by Poirier[18] to describe the symmetry of the TR Hamiltonian of $H_2@C_{60}$ under the assumption of rigid C_{60} molecules. To be consistent with these works, we will use equivalent notation in S_6 symmetry.

Having obtained symmetry-adapted TR-coupled states, we construct a potential from a linear combination of these states that is invariant under all operations of the required symmetry.[19] After further analysing the symmetries of the contributions to this potential, we will obtain analytical expressions for the matrix elements of the potential. We will then compare results using our po-

tential with both the results of the electrostatic interaction model and the results of our DFT calculations.

2 Derivation of symmetry-adapted states

In this section, we will define rotational and translational states that form a basis for the motion of a confined water molecule. We then show how projection operators can be used to construct linear combinations of products of these states that have $I_h^{(12)}$ and $S_6^{(12)}$ symmetries.

2.1 Translational and rotational states

As the cavity inside a C_{60} molecule is almost spherical, we will describe the translation of the centre of mass of an encapsulated water molecule using spherical polar coordinates $\{R_{\rm cm}, \theta_{\rm cm}, \phi_{\rm cm}\}$ defined relative to the centre of the C_{60} molecule. Rotation of the water molecule about its centre of mass can be described in terms of Euler angles $\{\phi, \theta, \chi\}$ relating the orientation of the water molecule relative to space-fixed axes $\{\xi, \eta, \zeta\}$ through the centre of mass of the water molecule. It is convenient to define molecule-fixed axes $\{x_w, y_w, z_w\}$ through the water molecule's centre of mass such that the water molecule lies in the x_w–z_w plane with its dipole axis (bisecting the $\widehat{\rm HOH}$ angle) along the z_w-axis, as shown in the inset to Fig. 1. The angles θ and ϕ define the orientation of the z_w-axis relative to the space-fixed coordinates. The angle χ defines the rotation of the water molecule about the z_w-axis, measured from the line defined by the intersection of the x_w–y_w and ξ–η planes, as also shown in Fig. 1. The dipole axis of the water molecule points towards the centre of the C_{60} molecule when $\{\theta = \theta_{\rm cm}, \phi = \phi_{\rm cm}\}$, and radially outwards from the centre of the C_{60} molecule when $\{\theta = \pi - \theta_{\rm cm}, \phi = \pi + \phi_{\rm cm}\}$.

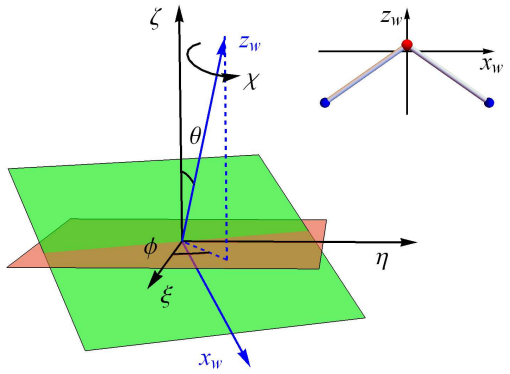

Fig. 1 Definition of Euler angles $\{\phi, \theta, \chi\}$, space-fixed axes $\{\xi, \eta, \zeta\}$ and molecule-fixed axes $\{x_w, z_w\}$. y_w is defined such that the molecule-fixed axes form a right-handed set. The inset shows the position of a water molecule in the molecule-fixed coordinate system. The centre of mass of the water molecule is at the origin of both coordinate systems. θ and ϕ define the orientation of the z_w axis, and χ determines the rotation of the water molecule about the z_w axis. χ is measured from the line formed by the intersection of the x_w–y_w and ξ–η planes (shown as pink and green squares respectively).[10]

The coordinates of a point $\{\xi, \eta, \zeta\}$ in the space-fixed coordinates through the centre of mass of the water molecule can be obtained from the coordinates $\{x_w, y_w, z_w\}$ in the molecule-fixed system by multiplying by the inverse of a matrix $A(\phi, \theta, \chi)$ that is a product of three Euler rotation matrices.†[10] Coordinates $\{x, y, z\}$ in a space-fixed system through the centre of a C_{60} molecule are then obtained by translating the origin.†

The Hamiltonian describing the translational motion, $\mathscr{H}_{\rm trans}$, and rotational motion, $\mathscr{H}_{\rm rot}$, of an encapsulated water molecule is

$$\mathscr{H}_{\rm T+R} = \mathscr{H}_{\rm trans} + \mathscr{H}_{\rm rot} \tag{1}$$

In our coordinate system, the principal axes $\{a, b, c\}$ of the water molecule (ordered such that a has the smallest moment of inertia and c has the largest) are equivalent to $\{x_w, z_w, y_w\}$, which is known as a II^l convention.[20] In this convention, the asymmetric top Hamiltonian can be written as[10]

$$\mathscr{H}_{\rm rot} = \hbar^{-2}\left(A_e \hat{J}_{x_w}^2 + C_e \hat{J}_{y_w}^2 + B_e \hat{J}_{z_w}^2\right) \tag{2}$$

where $\{\hat{J}_{x_w}, \hat{J}_{y_w}, \hat{J}_{z_w}\}$ are components of the rotational angular momentum about the $\{x_w, y_w, z_w\}$ axes, which can be written explicitly in terms of derivatives of the Euler angles $\{\phi, \theta, \chi\}$.†[10]

A_e, B_e and C_e are rotational constants, which are proportional to the inverse of the moment of inertia about the axes a, b and c. For a free water molecule, they are often given the values $A_e = 27.877$ cm^{-1}, $B_e = 14.512$ cm^{-1} and $C_e = 9.285$ cm^{-1} defined by Herzberg.[21] More recent *ab initio* calculations report values of $A_e = 27.8806$ cm^{-1}, $B_e = 14.5219$ cm^{-1} and $C_e = 9.27753$ cm^{-1} or, when centrifugal distortion is taken into account, $A_e = 27.8787$ cm^{-1}, $B_e = 14.5115$ cm^{-1} and $C_e = 9.28799$ cm^{-1}.[22] Values of $A_e = 27.2$ cm^{-1}, $B_e = 14.6$ cm^{-1} and $C_e = 9.5$ cm^{-1} have also been used.[10]

It is expected that the rotational constants will change upon encapsulation, as has been reported for other molecules.[23–25] Calculations have suggested that the water molecule experiences an increase in the H-O bond length upon encapsulation of between 0.0018 Å and 0.0026 Å,[4] or of around 0.0539 Å.[26] The $\widehat{\rm HOH}$ bond angle was found to decrease by between 0.57° and 0.87°,[4] or to increase by around 0.77°.[26] Our own DFT simulations indicate that the bond length increases by around 0.0005 Å and that the bond angle decreases by around 0.52°. Calculating values for the rotational constants by approximating the atoms in the water molecule to point masses at their equilibrium positions shows that all three rotational constants decrease as the bond length increases. whereas A_e decreases but B_e and C_e increase as the bond angle reduces. However, determination of effective values for the rotational constants for an encapsulated water molecule is more complex than this. The moments of inertia acquire effective mass from the fullerene cage,[25] and non-rigidity of the water molecule and anharmonicity of its vibrational motion both lead to vibrational-rotational interactions that introduce so-called centrifugal distortion constants.[10] Moreover, the rotational constants also change when the rotational motion is hindered by a small barrier, as is the case here.[27] Whilst expecting changes in the rotational constants upon encapsulation, we will use the values defined by Herzberg[21] to be consistent with the values used in the electrostatic interaction model.[14,28]

The rotational wavefunctions that are solutions to Eq. (2) are

linear combinations of symmetric top wavefunctions

$$\Phi_{\rm rot} = \sqrt{\frac{2J+1}{8\pi^2}} D^{(J)*}_{m,k}(\phi,\theta,\chi) \tag{3}$$

where the $D^{(J)*}_{m,k}(\phi,\theta,\chi)$ are complex conjugates of Wigner matrices whose explicit form is given in the ESI,† and m is a quantum number in the range $-J$ to $+J$. As $-J \le k \le J$ also, this means there are $(2J+1)^2$ rotational functions for each value of J.

For the translational motion, we will assume that the C_{60} molecule provides a cavity that can be approximated as spherical. Any deviations from spherical symmetry will be included via an additional symmetry-lowering potential acting within the spherical basis. The translational Hamiltonian is therefore

$$\mathscr{H}_{\rm trans} = -\frac{\hbar^2}{2m}\nabla^2 + V_{\rm trans} \tag{4}$$

where

$$V_{\rm trans} = \frac{1}{2} m\omega^2 R^2_{\rm cm} \tag{5}$$

is the translational potential energy, m is the mass of the water molecule and $\hbar\omega$ is the translational quantum. INS experiments[12] indicate that a water molecule encapsulated inside C_{60} has $\hbar\omega \approx 14$ meV. Felker and Bačić[17] obtained a value of 20.0967 meV, but this may involve some incorrect assignments of features in the experimental data of Goh *et al.*[12] We will set $\hbar\omega = 20.0967$ meV when comparing with the electrostatic interaction model, but treat it as a variable parameter whose value is expected to be in the range 14 to 20 meV when matching to our DFT results.

Eigenstates of the translational Hamiltonian in Eq. (4) can be written as[29]

$$\Psi_{\rm trans} = Y_{l,m}(\theta_{\rm cm},\phi_{\rm cm})\,\phi_{N_r,l}(R_{\rm cm}) \tag{6}$$

where the $Y_{l,m}(\theta_{\rm cm},\phi_{\rm cm})$ are spherical harmonics and

$$\phi_{N_r,l}(R_{\rm cm}) = N_{N_r,l} R^l_{\rm cm} {\rm e}^{-\nu R^2_{\rm cm}} L^{l+\frac{1}{2}}_{N_r}(2\nu R^2_{\rm cm}) \tag{7}$$

where $\nu = \frac{m\omega}{2\hbar}$, $L^{l+\frac{1}{2}}_{N_r}(2\nu R^2_{\rm cm})$ is a generalised Laguerre polynomial and $N_{N_r,l}$ is a normalisation constant given by

$$N^2_{N_r,l} = \sqrt{\frac{2\nu^3}{\pi}}\,\frac{2^{N_r+2l+3} N_r!\,\nu^l}{(2N_r+2l+1)!!} \tag{8}$$

These states have energies $(N+\frac{3}{2})\hbar\omega$, where $N = 2N_r + l$.

We will consider rotational states up to $J = 3$ and translational states up to $l = 3$, which gives a basis of 84 rotational states and 16 translational basis states for each value of N_r. However, we will only present explicit results up to $l = J = 2$ in our tables. It is a simple matter to include states up to arbitrary values of N_r because the $\phi_{N_r,l}$ are radial so do not affect transformations about the centre of the C_{60} molecule.

2.2 Projection operators

States that transform according to a given irreducible representation of a point group can be obtained using the method of projection operators.[30] Projection operators are defined as

$$\rho^{(i)}_{ts} = \frac{d_i}{g}\sum_R D^i(R)^*_{ts} R \tag{9}$$

where g is the order of the group, d_i is the dimension of a representation of symmetry Γ_i, R is an element of the group from which states are to be projected and $D^i(R)_{ts}$ is the tsth element of the matrix representation of R. A set of symmetry-adapted states can be obtained from a set of generating functions by operating with $\rho^{(i)}_{ts}$ on each generating function. The result will be a state transforming as Γ_i if the generating function forms part of that representation or zero if it does not.

The method of projection operators has previously been used to obtain symmetry-adapted vibronic states for $T\otimes(e+t_2)$ and $T\otimes h$ JT systems,[9,31] where the generating functions are products of electronic and vibrational states. In the current problem, the procedure is similar except that the generating functions are products of translational and rotational states.

When we apply symmetry operations to our translational and rotational basis states, we want to be able to write the new wavefunctions in terms of a linear combination of products of translational and rotational wavefunctions in our original basis set. In order to be able to do this analytically, care must be taken to avoid complicated expressions involving inverse trigonometric functions. Representation matrices $T_{1u}(R)$ that give the effect of each real rotation R of the I_h group on $\{x,y,z\}$ have been obtained previously.[32] To obtain results for S_6 symmetry, we start by using knowledge that in I_h symmetry, $\{x,y,z\}$ transform as T_{1u}. When the symmetry is reduced to S_6, the matrices $T_{1u}(R)$ for the operations that survive can be used to determine how $\{x,y,z\}$ transform in the reduced symmetry. However, the I_h matrices[32] were obtained for the case where $\{x,y,z\}$ are all C_2 axes of an icosahedron. Hence it is first necessary to change to a C_3 z-axis by rotating by an angle $\theta_v = \tan^{-1}(\frac{1}{2}(3+\sqrt{5}))$ in the x–z plane (see Fig. 1 in Hands *et al*[33]).

Applying the $T_{1u}(R)$ matrices to the Cartesian coordinates $\{x_{\rm cm}, y_{\rm cm}, z_{\rm cm}\}$ of the centre of mass gives new coordinates according to

$$\begin{pmatrix} x_{\rm cm} \\ y_{\rm cm} \\ z_{\rm cm} \end{pmatrix} \rightarrow T_{1u}(R) \begin{pmatrix} x_{\rm cm} \\ y_{\rm cm} \\ z_{\rm cm} \end{pmatrix} \tag{10}$$

for the identity and real rotations. For the inversion and improper rotation operations, the rotated coordinates need to be multiplied by -1. We can write the spherical harmonics in the translational states $\Psi_{\rm trans}$ in terms of simple algebraic combinations of $\{x_{\rm cm}, y_{\rm cm}, z_{\rm cm}\}$, plus factors containing $R_{\rm cm}$ that are unaltered by point group operations. As the radial functions in the translational states are functions of $R_{\rm cm}$, they do not need to be considered in this part of the calculation. Rewriting the results of applying the $T_{1u}(R)$ to the $\Psi_{\rm trans}$ in terms of linear combinations of the $\Psi_{\rm trans}$ is then only a matter of simple algebra.

The coordinates of the water molecule in a space-fixed coordinate system are related to those in a molecule-fixed system through the inverse of the matrix $A(\phi,\theta,\chi)$,† such that $A^{-1}(\phi,\theta,\chi) \rightarrow T_{1u}(R)A^{-1}(\phi,\theta,\chi)$ for the identity and real rota-

tions. For inversion and improper rotations, we must then make the replacements $\phi \to \phi + \pi$, $\theta \to \pi - \theta$ and $\chi \to \pi - \chi$. It is then a simple matter to write the rotational basis functions $\Phi_{\rm rot}$ for $J = 1$ in terms of elements of $A^{-1}(\phi, \theta, \chi)$, and hence to determine how these states transform under the operations R. For $J = 2$ and above, we can write products of two Wigner matrices in terms of a sum of single Wigner matrices using the relation

$$D^{(j)}_{m,k} D^{(j')}_{m',k'} = \sum_{J=|j-j'|}^{j+j'} \langle jmj'm'|JM\rangle \langle jkj'k'|JK\rangle D^{(J)}_{m+m',k+k'}, \qquad (11)$$

where $M = m + m'$ is the magnetic quantum number associated with the angular momentum J, $K = k + k'$ and the $\langle jmj'm'|JM\rangle$ are Clebsch-Gordan coefficients. Solving the equations backwards allows us to write Wigner matrices for higher J values in terms of products of Wigner matrices for lower J values. This means that results for higher J values can also be written in terms of the elements of $A^{-1}(\phi, \theta, \chi)$ without having to solve inverse trigonometric relations.

The S_6 group has singlet irreducible representations A_g and A_u, and doublet representations E_g and E_u. For the singlet representations, the representation matrices $D^i(R)$ are the same as the characters so can be looked up from character tables. For the doublets, we can then use the character tables to show that two pairs of orthogonal combinations of powers of $\{x, y, z\}$ that transform as E_g and E_u are $\{yz, -xz\}$ and $\{2xyz, z(y^2 - x^2)\}$ respectively, where z is a C_3 axis of the C_{60} molecule. The choice and phases of the orthogonal pairs is not unique; the choice given here ensures that the representations for proper rotations are the same for E_g and E_u. Applying the transformation of x, y and z under an operation R to these combinations using the $T_{1u}(R)$ matrices allows the required 2×2 matrices to be obtained.

The results of applying the projection operators is a set of symmetry-adapted states that transform according to the irreps. Γ_i of the appropriate group.† The parity of the states can be found by determining the effect of a permutation of the two H atoms, which involves changing $\chi \to \chi + \pi$ in the rotational wavefunctions. It is a straightforward matter to show that all of our results are automatically either symmetric or antisymmetric under this exchange.

3 TR-coupled energy levels

We will first determine analytical expressions for the matrix elements of $\mathscr{H}_{\rm T+R}$ in Eq. (1), which allows us to determine the energies of a H_2O molecule including translational and rotational terms only. We will then derive a general expression for a potential that can be used to describe the motion of a water molecule in environments of I_h and S_6 symmetries. We show that some contributions to this potential actually have a symmetry higher than the symmetry under consideration. We then show how analytical expressions for the matrix elements with the potential can be determined.

3.1 Energies excluding TR coupling

Symbolic expressions for the matrix elements of $\mathscr{H}_{\rm rot}$ between all rotational states can be obtained using orthogonality properties of the Wigner matrices.† The translational basis states are eigenstates of $\mathscr{H}_{\rm trans}$ so this contribution is easily incorporated. Hence a Hamiltonian matrix for $\mathscr{H}_{\rm T+R}$ in a basis consisting of the symmetry-adapted states can be constructed. This matrix is automatically block-diagonal, with each block corresponding to a specific component of an irrep. $\Gamma_i^{(p)}$ ($p = \{s, a\}$) of the symmetry group under consideration.

The eigenvalues associated with the lowest translational state in both S_6 and I_h symmetries are the same as those of a free water molecule (with no additional splittings). However, they can be labelled according to the irreps. $\Gamma_i^{(p)}$ rather than with the J_{k_a,k_c} notation. The equivalences between the two notations for some low-lying states are given in Table 1. The equivalencies between the J_{k_a,k_c} notation and irreps. of $I_h^{(12)}$ symmetry are the same as those reported previously.[28] They confirm that the 1_{01} level is not split in $I_h^{(12)}$ symmetry. All antisymmetric states are *ortho* states ($k_a + k_c$ odd) and all symmetric states are *para* states ($k_a + k_c$ even).

$J_{k_a k_c}$	$I_h^{(12)}$	$S_6^{(12)}$
0_{00}	$A_g^{(s)}$	$A_g^{(s)}$
1_{01}	$T_{1u}^{(a)}$	$A_u^{(a)} + E_u^{(a)}$
1_{11}	$T_{1u}^{(s)}$	$A_u^{(s)} + E_u^{(s)}$
1_{10}	$T_{1g}^{(a)}$	$A_g^{(a)} + E_g^{(a)}$
2_{02},2_{20}	$H_g^{(s)}$	$A_g^{(s)} + 2E_g^{(s)}$
2_{12}	$H_g^{(a)}$	$A_g^{(a)} + 2E_g^{(a)}$
2_{11}	$H_u^{(s)}$	$A_u^{(s)} + 2E_u^{(s)}$
2_{21}	$H_u^{(a)}$	$A_u^{(a)} + 2E_u^{(a)}$

Table 1 Correspondence between the labels J_{k_a,k_c} of an asymmetric top rotor and the irreps. of $I_h^{(12)}$ and $S_6^{(12)}$ symmetries for some of the low-lying levels.

3.2 Energies including TR coupling

We have already seen that in order to explain the experimentally-observed splitting in the 1_{01} level and other changes in the energies of the rotational levels that occur upon confinement of the water molecule inside C_{60}, a symmetry-lowering potential must be present. This will reflect coupling between the translational and rotational states. In general, the different irreps. in Table 1 that make up a given $J_{k_a k_c}$ level will then have different energies. Even in $I_h^{(12)}$ symmetry, levels with degeneracies higher than 5 (not shown in the table) will be split.

We will write the potential in terms of an expansion in the symmetry-adapted basis states. According to the basic laws of quantum mechanics, the Hamiltonian of any system must be invariant under all operations of the group to which the system it describes belongs,[19] which means that it must transform as the totally symmetric irrep. of the relevant group. We therefore take our potential to be a linear combination of our totally-symmetric symmetry-adapted states. These are the states that transform as $A_g^{(s)}$ in both $I_h^{(12)}$ and $S_6^{(12)}$ symmetries.† It should be noted that,

because the totally symmetric irreps. are (by definition) symmetric under exchange of the two H atoms, our potential does not mix *ortho* (antisymmetric) and *para* (symmetric) states. Other works that use knowledge that the Hamiltonian is invariant under all operations of the group to which it belongs include generation of a polynomial to represent a diabatic potential to describe vibronic coupling,[34] and derivation of the vibronic Hamiltonian for tetrahedral systems to arbitrary order.[35] It should be noted that our method is different to that used to model a hydrogen molecule encapsulated inside C_{60}.[36] That work employed an expansion in bipolar spherical harmonics and didn't use symmetry-adapted states.

We have obtained all states ψ_{i,N_r} in $I_h^{(12)}$ and $S_6^{(12)}$ symmetries up to $l = J = 3$, using a 2-fold z-axis for $I_h^{(12)}$ symmetry and a 3-fold z-axis for $S_6^{(12)}$ as these are the choices that give the simplest results. Although the derivation produces states of $A_g^{(s)}$ symmetry (in both cases), we will examine the symmetry properties of the states up to $l = J = 2$ further. There is one state (for each N_r) that depends only on the radial distance of the centre of mass ($R_{\rm cm}$), so it is immediately clear that this actually has the higher spherical symmetry, which is often called K_h symmetry.[18] There are three remaining contributions (for each N_r) in $I_h^{(12)}$ symmetry. It can be seen that these are symbolically the same as three contributions obtained in $S_6^{(12)}$ symmetry. At first sight, this appears unexpected because the $I_h^{(12)}$ states are expressed in terms of a 2-fold z-axis whilst the S_6^{12} states are in terms of a 3-fold z-axis. Further analysis of these combinations of states shows that they are invariant under arbitrary three-dimensional rotations about the centre of the C_{60} molecule. This means that they also have spherical symmetry.

Of the remaining contributions that don't occur in $I_h^{(12)}$ symmetry, we find that the only dependence on ϕ and $\phi_{\rm cm}$ in the contributions that are orthogonal to the spherical contributions, plus an additional four states (up to $l = J = 2$), is in the form $\phi - \phi_{\rm cm}$. Rotations about the z-axis by any angle involves changing ϕ and $\phi_{\rm cm}$ by the same amount. This means that these combinations are invariant under rotation by any angle about z. They are also invariant under inversion ($\theta_{\rm cm} \to \pi - \theta_{\rm cm}$, $\phi_{\rm cm} \to \phi_{\rm cm} + \pi$, $\theta \to \pi - \theta$, $\phi \to \phi + \pi$ and $\chi \to 2\pi - \chi$). This means that they actually have $D_{\infty h}$ symmetry (where their symmetry would be labelled as Σ_g^+), combined with symmetry upon permutation of the H atoms, which we will call $D_{\infty h}^{(12)}$ symmetry. They represent cases in which the water molecule sees an axial distortion due to the neighbouring (empty) C_{60} molecules, but where the angular positions of those molecules with respect to the distortion axis is not important. Because $D_{\infty h}^{(12)}$ symmetry only supports singlets and doublets, these terms will cause splittings of triplets (and higher degeneracies) in general.

The spherical and spheroidal results up to $l = J = 2$ are shown in Table 2 in terms of Wigner matrices $D_{m,k}^{(J)}(\phi,\theta,\chi)$, spherical harmonics $Y_{l,m}(\theta_{\rm cm},\phi_{\rm cm})$ and the radial functions $\phi_{N_r,l}(R_{\rm cm})$, where

$$D_{m,k}^{(J)\pm} = D_{m,k}^{(J)} \pm D_{m,-k}^{(J)} \tag{12}$$

and where

Symmetry	i	l	J	$4\pi V_{i,N_r}$
Spherical	1	0	0	$\sqrt{2}D_{0,0}^{(0)}Y_{0,0}\phi_{N_r,0}$
	2	1	1	$\frac{1}{\sqrt{3}}\left(\psi_{2,N_r}+\sqrt{2}\psi_{1,N_r}\right)$
	3	2	2	$\frac{1}{\sqrt{5}}\left(\psi_{7,N_r}+\sqrt{2}[\psi_{3,N_r}+\psi_{5,N_r}]\right)$
	4	2	2	$\frac{1}{\sqrt{5}}\left(\psi_{8,N_r}+\sqrt{2}[\psi_{4,N_r}+\psi_{6,N_r}]\right)$
Spheroidal	5	0	2	$\sqrt{5}D_{0,2}^{(2)+}Y_{0,0}\phi_{N_r,0}$
	6	0	2	$\sqrt{10}D_{0,0}^{(2)}Y_{0,0}\phi_{N_r,0}$
	7	1	2	$\sqrt{\frac{5}{2}}(D_{1,2}^{(2)-}Y_{1,1}-D_{-1,2}^{(2)-}Y_{1,-1})\phi_{N_r,1}$
	8	2	0	$\sqrt{2}D_{0,0}^{(0)}Y_{2,0}\phi_{N_r,2}$
	9	1	1	$\frac{1}{\sqrt{3}}\left(\sqrt{2}\psi_{2,N_r}-\psi_{1,N_r}\right)$
	10	2	2	$\frac{1}{\sqrt{2}}\left(\psi_{3,N_r}-\psi_{5,N_r}\right)$
	11	2	2	$\frac{1}{\sqrt{2}}\left(\psi_{4,N_r}-\psi_{6,N_r}\right)$
	12	2	2	$\frac{1}{\sqrt{5}}\left(2\psi_{7,N_r}-\frac{1}{\sqrt{2}}[\psi_{3,N_r}+\psi_{5,N_r}]\right)$
	13	2	2	$\frac{1}{\sqrt{5}}\left(2\psi_{8,N_r}-\frac{1}{\sqrt{2}}[\psi_{4,N_r}+\psi_{6,N_r}]\right)$

Table 2 Contributions V_{i,N_r} to a potential derived from $A_{1g}^{(s)}$ symmetry-adapted states up to $l = J = 2$ that actually have spherical ($K_h^{(12)}$) and spheroidal ($D_{\infty h}^{(12)}$) symmetry. The values in the table should be divided by 4π in order to obtain contributions involving normalised states.

$$\begin{aligned}
\psi_{1,N_r} &= \sqrt{3}(D_{1,0}^{(1)}Y_{1,1} + D_{-1,0}^{(1)}Y_{1,-1})\phi_{N_r,1}\\
\psi_{2,N_r} &= \sqrt{6}D_{0,0}^{(1)}Y_{1,0}\phi_{N_r,1}\\
\psi_{3,N_r} &= \sqrt{\tfrac{5}{2}}(D_{2,2}^{(2)+}Y_{2,2} + D_{-2,2}^{(2)+}Y_{2,-2})\phi_{N_r,2}\\
\psi_{4,N_r} &= \sqrt{5}(D_{2,0}^{(2)}Y_{2,2} + D_{-2,0}^{(2)}Y_{2,-2})\phi_{N_r,2}\\
\psi_{5,N_r} &= \sqrt{\tfrac{5}{2}}(D_{1,2}^{(2)+}Y_{2,1} + D_{-1,2}^{(2)+}Y_{2,-1})\phi_{N_r,2}\\
\psi_{6,N_r} &= \sqrt{5}(D_{1,0}^{(2)}Y_{2,1} + D_{-1,0}^{(2)}Y_{2,-1})\phi_{N_r,2}\\
\psi_{7,N_r} &= \sqrt{5}(D_{0,2}^{(2)} + D_{0,-2}^{(2)})Y_{2,0}\phi_{N_r,2}\\
\psi_{8,N_r} &= \sqrt{10}D_{0,0}^{(2)}Y_{2,0}\phi_{N_r,2}
\end{aligned} \tag{13}$$

are unnormalised $A_g^{(s)}$ states (that should be divided by 4π to get normalised states).

When used as part of a potential, the spherical contributions split some of the higher excited states compared to those of a free rotor, and alter the energies of all states (in general), but the degeneracies of lower-lying states are the same as those of a free rotor. In particular, they don't cause any triplets to split into doublets and singlets (because neither icosahedral or spherical symmetry supports doublet representations), so can't explain the splitting of the 1_{01} rotational level.

The remaining contributions up to $l = J = 2$ that do not appear in $I_h^{(12)}$ symmetry can be divided into five contributions that also appear if the calculations are repeated for $D_{3d}^{(12)}$ symmetry, and 12 contributions that only occur in $S_6^{(12)}$ symmetry.† We have also obtained results including $l = 3$ and/or $J = 3$, where, for example, we find that there are four spherical contributions with $l = J = 3$. These contributions are not presented here as their form is rather

complex.

As a result of the analysis above, our final result for the terms in the potential that occur in both $I_h^{(12)}$ and $S_6^{(12)}$ symmetries can be written in as

$$V = V_{\rm sph} + V_{D_{\infty h}} \tag{14}$$

where, up to $l = J = 2$,

$$V_{\rm sph} = \sum_{i=1}^{4} \sum_{N_r} k_{i,N_r} V_{i,N_r} \tag{15}$$

adds in spherically-symmetric contributions and

$$V_{D_{\infty h}} = \sum_{i=5}^{13} \sum_{N_r} k_{i,N_r} V_{i,N_r} \tag{16}$$

adds in the $D_{\infty h}^{(12)}$ contributions. The extra terms that occur in $S_6^{(12)}$ symmetry can be added to Equation (14) if required although, as we show later, the additional terms do not appear to be relevant in explaining the 1_{01} splitting. Similarly, terms with higher values of l and J can also be included if required.

Analytical expressions for matrix elements of the potential V between different translational and rotational basis states, and hence between symmetry-adapted states, can be obtained using additional relations between products of Wigner matrices and of spherical harmonics.† Within our basis of symmetry-adapted states, the result is still a block-diagonal matrix, with one block for each component of each irrep., as was the case before V was included. Each block can be separately diagonalised to obtain energies of the TR-coupled states subject to the symmetry-lowering potential. The symmetry labels that each state corresponds to are automatically retained. The degeneracies of all states are as expected from Table 1, with all triplets being split into singlets and doublets in $S_6^{(12)}$ symmetry for example.

4 Comparison with other theoretical models

As our potential V in Eq. (14) has been obtained using symmetry considerations alone, the k_{i,N_r} are unknown coefficients. Different values for the coefficients will describe different interactions. To show that our potential is indeed suitable for explaining the dynamics of a water molecule encapsulated in a fullerene molecule, we will first compare our results with those of the model that includes electrostatic interactions between the water molecule and the electron clouds of neighbouring fullerene molecules,[13,14] where the symmetry of the cluster under consideration is S_6. To further show validity of our model, we will then show that it can be used to reproduce DFT results obtained when a water molecule moves inside the cavity of an isolated (and undistorted) C_{60} molecule.

4.1 Comparison with electrostatic interaction model

The spherical terms V_{1,N_r} change the relative energies of the TR-coupled states but do not cause any splittings. The terms V_{2,N_r}–V_{4,N_r} lift degeneracies of some of the higher excited states to result in odd values for the degeneracies consistent with expectations for angular momentum states. However, none of the lower-lying states that are clearly resolved in INS have sufficiently high degeneracies for any splittings by these terms to be apparent. However, the $D_{\infty h}^{(12)}$ terms V_{5,N_r}–V_{13,N_r} lift all degeneracies greater than two-fold, as singlets and doublets are the only degeneracies allowed in this symmetry. More specifically, states with $m = 0$ form singlets and those with the with $\pm m$ ($m \neq 0$) form doublets.

The effect of some of the terms in V is negligibly small, especially terms that only mix states that are well-separated in energy, such as those involving different translational states. Further information on the contributions of different terms can be deduced by studying the symbolic forms of the V_{i,N_r} and the states. For example, the spherically-symmetric terms V_{1,N_r} are only functions of $R_{\rm cm}$. Therefore, their effect within a set of eigenstates belonging to the same translational level is to contribute a constant to each diagonal matrix element and hence to alter the relative positions of states associated with different translations but not alter the relative positions of different rotational states associated with the same translation.

The rules of angular momentum coupling allow us to make further predictions of the effect of the V_{i,N_r}. A general term in V_{i,N_r} contains products of Wigner matrices for an angular momentum $\mathbf{J}$ and spherical harmonics of angular momentum $\mathbf{l}$ in the form

$$v_\lambda = \lambda\, D^{(J)}_{m_J,k_J}\, Y_{l,m_l}\, \phi_{N_r,l} \tag{17}$$

where λ is a numerical factor. $D^{(J)}_{m_J,k_J}$ and $Y_{l,m_l}\,\phi_{N_r,l}$ add in interactions between rotational and translational states respectively. Two states ψ_μ and ψ_ν with angular momenta $\{\mathbf{l}_\mu,\mathbf{J}_\mu\}$ and $\{\mathbf{l}_\nu,\mathbf{J}_\nu\}$ can only interact via v_λ if vector triangles can be formed from both $\{\mathbf{l}_\mu,\mathbf{l}_\nu,\mathbf{l}\}$ and $\{\mathbf{J}_\mu,\mathbf{J}_\nu,\mathbf{J}\}$, i.e. if $|l_\mu - l_\nu| \leq l \leq l_\mu + l_\nu$ and $|J_\mu - J_\nu| \leq J \leq J_\mu + J_\nu$. Moreover, the conditions $m_{J_\mu} + m_{J_\nu} = m_J$, $k_{J_\mu} + k_{J_\nu} = k_J$ and $m_{l_\mu} + m_{l_\nu} = m_l$ relating the quantum numbers must also be obeyed. Therefore, only terms in the potential with $l = 0$ can interact within the lowest translational states ($l_\mu = l_\nu = 0$). Higher-order terms in the potential only contribute via off-diagonal mixing involving higher excited translational states, which will be small.

As a result of the above arguments, we can see that the effect of V is simplified significantly if we only consider couplings within the ground translational states ($N = 0$). More specifically, we find that only V_{1,N_r}, V_{5,N_r} and V_{6,N_r} have non-zero matrix elements, and as the V_{1,N_r} cause a constant shift to all of these energy levels, they can be neglected when analysing energy differences. Furthermore, matrix elements involving states with the same values of l and J but different values of N_r only differ because of the values of integrals involving the different $\phi_{N_r,l}$, which are related by simple numerical constants, e.g. $\langle\phi_{0,0}|\phi_{0,0}|\phi_{0,0}\rangle = \sqrt{6}\langle\phi_{0,0}|\phi_{1,0}|\phi_{0,0}\rangle$. Therefore, the effect of the potential on matrix elements involving the lowest translational state can be written in terms of the two parameters

$$a_i = k_{i,0} + \frac{1}{\sqrt{6}}k_{i,1} + \frac{\sqrt{5}}{6\sqrt{6}}k_{i,2} + \frac{\sqrt{35}}{108}k_{i,3} + \frac{\sqrt{35}}{216\sqrt{2}}k_{i,4} + \ldots \tag{18}$$

for $i = 5, 6$. These terms represent a spheroidal distortion. There

are no spherical terms that have any effect when considering the lowest translation only. When higher translational states are included, additional coefficients k_{i,N_r} do have an effect on the calculated energies.

In order to match the energy levels reported using the electrostatic interaction model,[13,14] we need to use the free-water rotational constants[21] and a translational quantum of 20.1 meV used in these works.†Column (a) of Figure 2 shows a close match to the results of the electrostatic interaction model (reproduced in column (c)) up to ≈ 12 meV, when only states corresponding to the lowest translation are considered. This was produced with two free parameters only, namely $a_5 = -0.6$ and $a_6 = 0.02$. The match with the levels at ≈ 17–18 meV is not so good. This is not surprising because as this result was obtained by considering the lowest translational states only, it would be expected to start to break down as the energies of the states start to approach the translational quantum of ≈ 20 meV. When translational excited states are included, extra coefficients k_{i,N_r} have an effect on the results. Column (b) shows results obtained with $a_5 = -0.63$, $a_6 = 0.04$ and $k_{1,2} = 4$, with all other coefficients being zero. The INS results[12,37] are shown in column (d) for comparison purposes.

Some differences remain between our results and those of the electrostatic interaction model, most notably that the levels attributed to 2_{21} and 2_{20} are higher in energy. The differences are because many additional contributions can affect the results when higher translational states are included. We have not included these terms in the results presented here for simplicity, in order to restrict the number of free parameters to be considered. The fact that we have been able to reproduce the splitting of the 1_{01} level with only spheroidal distortion terms shows that it is actually the fact that the cluster of neighbouring C_{60} molecules has a 3-fold axis of symmetry that is important for producing the splittings, not the fact that the system is only invariant with respect to 3-fold (proper and improper) rotations about that axis.

Analysis of the INS data by the original authors indicates that transitions to the 1_{10} and 2_{11} levels are either forbidden or too weak to be observed, or they are obscured by stronger transitions of similar energies[12,37]). Figure 2 shows the energies of the 1_{10} and 2_{11} levels for gaseous water.[37] For clarity, the symmetry labels for the states has not been given, but our procedure does automatically label the states. It has been shown that in spherical symmetry, transitions for which the Kronecker product of the symmetries of the initial and final state doesn't contain S_g, P_u, D_g, F_u ... are forbidden[18]. However, it is not known what transitions will be sufficiently strong for the relevant levels to be observed when the symmetry has been distorted to spheroidal.

There are discrepancies between the INS results and those of the electrostatic interaction model. We can choose parameters in our model, including modified values for the rotational constants (which, as mentioned previously, are expected to change upon encapsulation), that give closer matches to at least some of the INS results, which may indicate that another interaction could also be contributing to the symmetry-lowering. However, the resolution of the current INS data is insufficient for any concrete conclusions to be drawn. Although the energies of the INS levels were quoted to have errors of ± 0.05 meV, ± 0.1 meV or ± 0.2 meV (depending upon the instrument used to observe the level),[12,37] the actual results form bands that almost certainly contain unresolved splittings. Further experimental results that resolve splittings of levels higher than 1_{01} are required before this can be pursued any further.

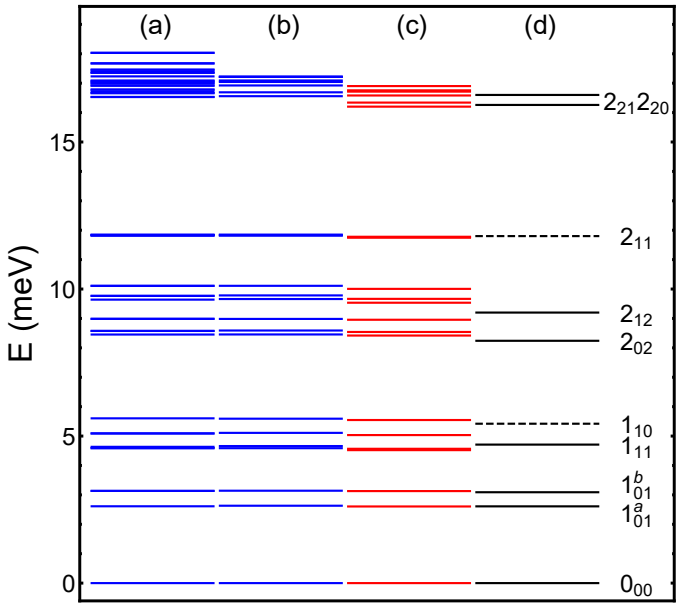

Fig. 2 Column (c) shows the results obtained by Bačić *et al.*[14] Column (a) shows a match to the results in (c) that we have obtained considering states associated with the lowest translational state only. Column (b) shows an alternative match obtained when higher translational states are included. Column (d) shows the experimental energies obtained from INS.[12,37] The 1_{10} and 2_{11} levels are not resolved in the INS data; values for gaseous water[37] are shown here as dashed lines.

It has been seen that the 1_{01} level splits into a lower singlet and higher doublet[12] (although the doublet was inadvertently reported as being lowest in Goh *et al*[38]) such that

$$\begin{aligned} E_1 - E_g &\approx 2.61 \text{ meV} \\ E_2 - E_g &\approx 3.09 \text{ meV} \end{aligned} \tag{19}$$

were E_g is the energy of the 0_{00} ground state, and E_1 and E_2 are the energies of the singlet and doublet components of 1_{01} respectively. As can be seen in Fig. 2, the energies of these levels can be determined to a good approximation by considering only the lowest translational state. In fact, the energies can be obtained from the rotational states associated with this translation up to $J = 2$ only. Table 1 shows that the singlet component of the 1_{01} level transforms as $A_u^{(a)}$. As we have used basis states appropriate to $S_6^{(12)}$ symmetry, our Hamiltonian matrix is automatically divided into separate blocks for each irrep. This shows that there is only one state transforming as $A_u^{(a)}$ within the relevant basis states. Its energy must therefore equal E_1. Likewise, we can see that there are three $A_g^{(s)}$ states that could match the 0_{00} level, so E_g comes from the lowest root of a 3×3 matrix. Similarly, there are two $E_u^{(a)}$ states that could match the doublet component of 1_{01}, so E_2 comes from the lowest root of a 2×2 matrix. Matching both energy gaps in Eq. (19) gives two equations in two unknowns (a_5 and a_6) for fixed values of the rotational constants, although some

variation in the values should be allowed because the energy gaps are subject to experimental uncertainties. This shows that there is a range of pairs of a_5 and a_6 that match the splitting of the 1_{01} level and the differences between these energies and those of the ground (0_{00}) state. This is confirmed by our calculations. The energies of the states above 1_{01} are different for different pairs of a_5 and a_6 though. However, in all cases, the 1_{11} and 1_{10} states split such that a doublet is lowest and a singlet highest, even though the 1_{01} state has a singlet lowest and a doublet highest.

4.2 Match to DFT

To further confirm that our model can represent the dynamics of an encapsulated water molecule, we will show that our model can provide a good match to the results of DFT calculations in which an encapsulated water molecule moves inside the cage of an isolated C_{60} molecule. We assume that the C_{60} cage is a rigid structure with icosahedral symmetry, which means that it is only the terms obtained by carrying out our calculations in icosahedral symmetry that are relevant. As we have seen previously, these terms all turn out to have the higher spherical symmetry, rather than actually having icosahedral symmetry. This means that it is the fact that the Carbon atoms in C_{60} all lie on the surface of a sphere that is relevant, with the placement of the Carbon atoms on that sphere being irrelevant at this level of approximation.

To obtain results which we can use with our model, we have performed DFT calculations on $H_2O@C_{60}$ molecules using the hybrid Gaussian and plane waves method (GPW) as implemented in the CP2K package.[39] The simulations employed Perdew, Burke and Enzerhof (PBE) exchange-correlation functionals and Goedecker-Teter-Hutter (GTH) pseudopotentials[40] to replace the atomic cores of all C, H and O atoms together with their optimised TZV2PX-MOLOPT pseudo wave functions.[41] The calculations were performed in the Quickstep module of CP2K. In order to account for non-covalent interactions between the host and guest molecules, the DFT-D3 long-range correlation correction of Grimme[42] was employed. The energy cut-off for the plane wave expansion was set at 1300 Ry as found by optimization. The simulated molecule was placed in a $20\times20\times20$ Å simulation box.

While DFT results give the energy of the system as a whole and not the potential, we expect the changes in energy as a function of position and orientation of the water molecule to be predominantly related to changes in the potential. We will therefore equate the results to a potential energy surface (PES). We therefore started our calculations by obtaining relaxed geometries of H_2O and of C_{60} in isolation according to the level of theory we used. We then calculated the energies for various positions of the water molecule relative to the C_{60} cage without allowing the water or fullerene molecule to further relax. This is because we do not wish to determine the minimum energy, and also because we want the changes in energy to relate to the spherical terms in our potential alone.

Due to resource implications, it is not feasible to perform DFT calculations covering the complete six-dimensional parameter space comprised of the centre of mass coordinates $\{R_{\rm cm}, \theta_{\rm cm}, \phi_{\rm cm}\}$ and the Euler angles $\{\phi, \theta, \chi\}$. The cavity inside the C_{60} molecule is almost spherical, and to a first approximation, the water molecule will see a potential equivalent to averaging the discrete positions of the Carbon atoms over the surface of a sphere. This means that we expect any variation in the potential as the water molecule moves such that $R_{\rm cm}$ is a constant will be very small. The variation in the potential as $R_{\rm cm}$ varies will be considerably larger (> 150 meV between the cage centre and cage wall). Also, changes due to rotations of the water molecule about the dipole axis are very small. Therefore, we will determine the variation in energy as the centre of mass of the water molecule traverses along several different radial axes through the centre of the fullerene molecule, keeping the other coordinates constant. Any differences depend predominantly on the choice of the radial axis and the orientation of the dipole axis of the water molecule with respect to that axis. We have investigated cases where the dipole axis is parallel to a C_2, C_3 or C_5 axis of the (undistorted) C_{60} molecule, as well as an axis along the direction from the centre of the cage to a single bond (joining a hexagon and a pentagon).

As we want to compare results for different orientations of the dipole axis of the water molecule, it is convenient here to choose our space-fixed axes through the centre of the C_{60} molecule to all be C_2 axes. As the spherically-symmetric terms have the same symbolic form irrespective of the definition of the z-axis, we can use the same expressions to compare different orientations. We choose the dipole axis to lie in the x–z plane at an angle θ_v to the z-axis (as defined in Section 2.2). This means that the Euler angles are $\theta = \theta_v$ and $\phi = 0$. We also choose $\chi = 0$.

Firstly, we obtain results in which the centre of mass of the water molecule moves along the space-fixed x-axis. Figure 3 shows the variation in DFT energy (with respect to an arbitrary zero of energy) as a function of the distance $x_{\rm cm}$ of the centre of mass of the water molecule from the centre of the C_{60} molecule when the dipole axis is parallel to a C_2 axis (red squares) or C_5 axis (blue circles). For clarity, points have been shown in steps of 0.04 Å, whereas the full data contains points in steps of 0.02 Å. When the dipole axis is parallel to a C_2 axis, the DFT results are symmetric about $x_{\rm cm} = 0$ because the geometries of the $H_2O@C_{60}$ system at positive and negative values of $x_{\rm cm}$ are mirror images of each other. When the dipole axis is parallel to a C_5 axis, there is a small antisymmetric component to the PES because the geometries at positive and negative values of $x_{\rm cm}$ are not equivalent.

Figure 4 shows similar results to figure 3 but when the centre of mass moves along the z-axis. Results when the dipole axis is parallel to a radial axis towards a single bond are almost identical to those when it is a C_5 axis (with a maximum difference of 1.8 meV) so they are not presented here. Similarly, the results when the dipole axis is parallel to a C_3 axis are not presented as they are almost identical to those when it is a C_2 axis, with a maximum difference of ~ 0.3 meV near to the minimum and up to 10 meV at values furthest away from the minimum. There is a much larger antisymmetric component for all orientations than for when the centre of mass moves along the x-axis. The least energy occurs when the dipole axis points towards the cage centre with the centre of mass is 0.096 Å from the cage centre. This corresponds to a displacement of 0.16 Å in the position of the O atom from the cage centre. The energy barrier between when the O atom is at

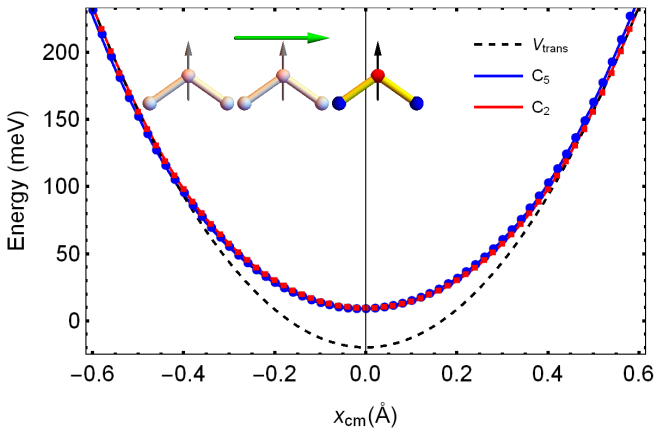

Fig. 3 Variation in the DFT energy of an encapsulated water molecule when its dipole axis is aligned along a z-axis which is parallel to a C_5 axis (blue circles) and a C_2 axis (red squares) of a C_{60} molecule and the centre of mass of the water molecule traverses along the x direction, as illustrated by the inset. The solid lines give the corresponding fits to the potential V_{tot}, and the (black) dashed line gives the result for the parabolic potential V_{trans}. All results are relative to an arbitrary zero in energy.

0.16 Å and when it is at the centre of the cage is ~ 11.25 meV. All of these results are in line with results reported previously.[4,43] For example, Varadwaj and Varadwaj[4] also reports a potential with a significant antisymmetric component, although their potential is flatter around the minimum energy. This maybe due to the different level used for their DFT calculations, or because the only parameter they constrained at each point on their curve was the distance of the O atom from the centre of the C_{60} cage whereas we (by design) constrained both the geometry of the C_{60} molecule and that of the water molecule.

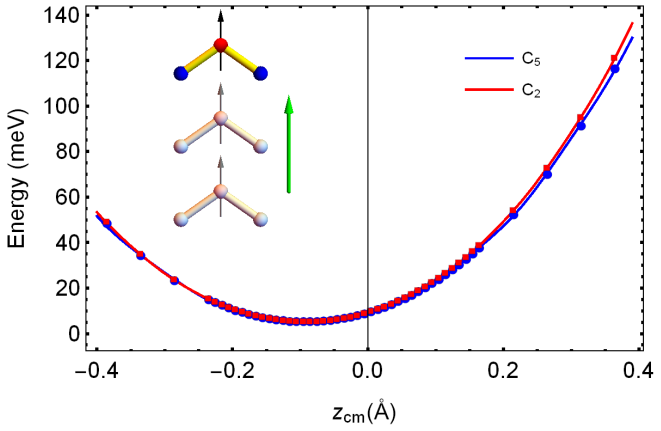

Fig. 4 As for figure 3 but where the centre of mass of the water molecule traverses along the z direction.

From Fig. 3, we can see that the results for different orientations of the dipole axis of the water molecule with respect to the C_{60} molecule are very similar as long as the centre of mass moves in a direction perpendicular to the dipole axis. Similarly, Fig. 4 shows that the results are also very similar when the centre of mass moves along the same direction as the dipole axis. This is not surprising because all of the carbon atoms lie on a sphere with the only difference being in the positions of the atoms relative to the z-axis. The average effect of all 60 carbon atoms is very similar in all cases.

It should be noted that the fact that the minimum energy in Fig. 4 is not at $z_{cm} = 0$ is consistent with the results of previous calculations, which have shown a shift in the position of the O atom from the cage centre of between ~ 0.1 and 0.3 Å,[4] around 0.05 Å,[26] or 0.16 Å.[43] with a small energy barrier between the minimum-energy position and cage centre in all cases. However, our results don't relate directly to these results because we constrained our C_{60} molecule to retain its icosahedral symmetry so that we could evaluate the effect of the spherical terms in our potential.

Having obtained results for an effective PES using DFT, we now need to determine whether we can explain the DFT results using the total potential

$$V_{tot} = V_{trans} + V_{sph} \tag{20}$$

where the parabolic translational potential V_{trans} in equation (5) is the dominant contribution and the potential V_{sph} has a much smaller effect.

To proceed, we note that along our DFT profiles in Fig. 3, we have $\theta_{cm} = \theta_v + \pi/2$ and $\phi_{cm} = 0$ when moving along the positive x-axis but $\theta_{cm} = \pi/2 - \theta_v$ and $\phi_{cm} = \pi$ when moving along the negative x-axis. Examining the forms of the contributions to the potential with these angles shows that the results for negative x can be obtained from those for positive x by replacing R_{cm} by $-R_{cm}$. This is equivalent to writing the results in terms of the Cartesian x-coordinate of the centre of mass, x_{cm}, in a reference frame in which the dipole axis is along the z-axis. More specifically, the potential V_{sph} can be written in terms of the product of an exponential factor $\exp(-\nu x_{cm}^2)$ and a polynomial in $\sqrt{\nu}x_{cm}$.

Similarly, for the profiles in Fig. 4, we have $\theta_{cm} = \theta_v$ and $\phi_{cm} = 0$ when the centre of mass of the water molecule moves along the positive z-axis and $\theta_{cm} = \pi - \theta_v$ and $\phi_{cm} = \pi$ when it moves along the negative z-axis. As a result, the potential can be written in terms of $\exp(-\nu z_{cm}^2)$ and a polynomial in $\sqrt{\nu}z_{cm}$ where z_{cm} is the Cartesian z-coordinate of the centre of mass in a frame in which the dipole axis is along z.

For both the x and z profiles, even values of l contribute even powers in the polynomial and odd values of l contribute odd powers. It is therefore convenient to fit the DFT profiles to an appropriate exponential and polynomials and then rewrite the results in terms of combinations of the $\phi(N_r, l)$, although a fit involving the $\phi(N_r, l)$ can be done directly.

As the exponential factor in V_{sph} decays to zero as we move away from the origin, the DFT results away from the origin must be dominated by the parabolic contribution V_{trans}. We start by considering the C_2 profile in figure 3 as this only contains symmetric contributions. A good fit to the dependence further away from the origin can be obtained if we take $\hbar\omega = (18.1 \pm 0.1)$ meV, which is within the expected range of 14 to 20 meV. This is shown as a (black) dashed line in figure 3. We will therefore take a value of 18.1 meV in the remainder of this section, although small changes in this value have very little effect on the results overall.

We can see that the DFT potential is flatter near the centre of the C_{60} cage than would occur due to a parabola alone. The difference between the DFT potential and the parabola in all of our profiles must be due to $V_{\rm sph}$, which we know contributes nearer to the origin. Figures 3 and 4 show the result of fitting our potential $V_{\rm tot}$ (as solid lines). It can be seen that all of the DFT results can be reproduced very accurately by our potential.

Rewriting our polynomial fits in terms of the original $\phi(N_r, l)$ and ensuring the fits to the different directions are consistent yields unique values for most of the contributing coefficients k_{i,N_r}, although a few of the coefficients for excited terms can be written in terms of non-unique linear combinations of other coefficients.

5 Discussion

The splitting of the 1_{01} level in $H_2O@C_{60}$ can be viewed as an example of a tunnelling splitting. When the water molecule is at positions that are equivalent from a symmetry point of view, the energy must be the same. This means that there are equivalent minima in the PES. If there were infinitely large barriers between the minima, the TR-coupled states associated with the minima would not interact; these states would be states of the system as a whole, and there would be no splittings. However, as the barriers are finite, the system can tunnel between the equivalent minima. States of the system are linear combinations of the states associated with the minima that reflect the symmetry of the system as a whole. The symmetry-adapted states group into states of different symmetries, which also have different energies. The situation is similar to that for water clusters where, drawing on early work by Longuet-Higgins,[44] interference between rovibronic wavefunctions associated with equivalent minima also results in the occurrence of tunnelling splittings.[45–47] It is also the same situation that occurs in the dynamic Jahn-Teller effect, except that here we have TR-coupled states rather than states coupling electronic and vibrational motion (and where the higher-energy components were sometimes called inversion levels[9]).

We have matched our energies with results of the electrostatic interaction model,[13,14] which included reproducing the splitting of the 1_{01} level seen experimentally in INS. Previous papers have suggested that JT distortions of the C_{60} cages could be at least partly responsible for the symmetry-lowering.[12,16] Indeed, JT and geometric factors have been used to explain the NMR spectra of $HF@C_{60}$,[25] As there isn't exact agreement between the result of the electrostatic interaction model and those of INS, it is certainly possible that JT effects could also be present. Indeed, at any instant in time, the C_{60} cage of an isolated fullerene ion will be distorted due to the dynamic JT effect.[9,48–53] However, while the instantaneous symmetry is lowered, the C_{60} cage will interconvert between equivalent minima on a rapid timescale (the order of pico to femto seconds[54]). It seems unlikely that the water molecule would be able to follow the distortions on this timescale such that it 'sees' the distorted geometry. Furthermore, for the mechanism to be due to JT effects, the C_{60} cage must be charged. There are no JT distortions in neutral C_{60} molecules as the highest occupied molecular orbital is completely full, so there would be no energy gain if the neutral C_{60} molecule were to distort. Calculations on single $H_2O@C_{60}$ molecules indicate that there is a charge transfer to the C_{60} cage upon encapsulation of a water molecule, although the extent of the charge transfer depends strongly on the method used. Various charge population analyses at the PBE0/6–311++G(d,p) level indicate that the charge transferred to the C_{60} cage is between $0.01e$ and $0.611e$,[4] whereas calculations at the B3LYP/6-31G** level indicate that the charge transfer is $0.19e$.[55] Therefore, although the possibility that the charge transfer is sufficient to induce JT distortions can't be ruled out, it seems unlikely that JT effects in isolated $H_2O@C_{60}$ molecules could be responsible for the observed reduction in symmetry. However, cooperative JT interactions between neighbouring C_{60} ions can result in distortions of individual C_{60} molecules being locked in place, resulting in static distortions of the individual molecules.[56–58] (This is different to an overall uniaxial distortion, because distortions of individual molecules will not be in the same directions.) The charge transfer in clusters of $H_2O@C_{60}$ molecules is unknown.

Our results show that common terms appear in the symmetry-lowering potential for both S_6 and D_{3d} symmetries. An important consequence of this is that it is possible for JT distortions of the C_{60} cages to D_{3d} symmetry to be present in addition to the electrostatic interactions with nearest neighbours (as long as the 3-fold distortion axes of the individual C_{60} cages are aligned such that when nearest-neighbours are taken into account the 3-fold symmetry of the overall system is preserved). However, further high-resolution measurements are required before any further conclusions can be made. It would be particularly interesting if it were possible to carry out experiments on endohedrally-doped A_nC_{60} fullerides, where the addition of alkali metal atoms A results in JT distortions of the C_{60} cages.[59–65]

6 Conclusions

We have developed a potential that can be used to model the interactions between a water molecule encapsulated in a C_{60} cage and its environment. Our potential is expressed in terms of linear combinations of translational and rotational basis functions. This totally general form must be able to describe the effect of any interaction that has the symmetry under consideration, with different interactions resulting in different values for the coefficients in our potential. When we consider rotational levels associated with the lowest translation only, we have shown that it is possible to choose values for the coefficients that result in energies up to ≈ 12 meV that are very similar to those of the electrostatic interaction model.[13,14] These results are obtained with two unknown parameters only, and do not require carrying out time-consuming calculations, such as the DFT calculations that were carried out in order to find the potential in the electrostatic interaction model.[14] Furthermore, our model shows that the terms in our potential that produce these results are actually invariant with respect to rotations by any angle about the 3-fold symmetry axis, having $D_{\infty h}$ symmetry rather than the S_6 symmetry that represents the actual geometry of the cluster of $H_2O@C_{60}$ molecules considered by this model. Addition of excited translational states is necessary in order to match the energies of higher excited states. This is to be expected for states whose energies are approaching the translational quantum.

We have also shown that our potential is able to explain the variation in energy seen in DFT as a water molecule traverses along radial directions inside an undistorted cage of an isolated C_{60} molecule, where the symmetry of the environment seen by the water molecule is icosahedral. In fact, it is a simple matter to use our approach to obtain results for any point group symmetry that is a subgroup of icosahedral symmetry. As our perturbing potential is an algebraic expression (in terms of the coordinates of the centre of mass of the water molecule and the Euler angles defining its orientation), it will be much easier to use the results in further calculations than using the DFT results directly.

There are still some discrepancies between the results obtained using the electrostatic interaction model and the INS results,[12,37] which could indicate that there are further interactions between the water molecule and its environment, such as JT or crystal field-type effects. Our model can obtain a closer match to at least some of the energies deduced from INS, but the resolution of the data is insufficient for us to make any concrete conclusions at the current time. This will be possible in the future if more data becomes available. Also, the same method we have presented here could be used to obtain the perturbing effect of the C_{60} cage on other molecules encapsulated inside a C_{60} molecule.

Conflicts of interest

There are no conflicts to declare.

Acknowledgments

The authors wish to thank Dr Salvatore Mamone and Prof Anthony J Horsewill for helpful discussions on this work. ER is grateful for funding from Umm Al-Qura University. We also acknowledge the support of the University of Nottingham High Performance Computing Facility (in particular, Dr Colin Bannister).

References

1 K. Kurotobi and Y. Murata, *Science*, 2011, **333**, 613–616.
2 S. Mamone, M. Concistrè, E. Carignani, B. Meier, A. Krachmalnicoff, O. G. Johannessen, X. Lei, Y. Li, M. Denning, M. Carravetta, K. Goh, A. J. Horsewill, R. J. Whitby and M. H. Levitt, *J. Chem. Phys.*, 2014, **140**, 194306.
3 D. Bucher, *Chem. Phys. Lett.*, 2012, **534**, 38–42.
4 A. Varadwaj and P. R. Varadwaj, *Chem. Eur. J.*, 2012, **18**, 15345–15360.
5 S. Aoyagi, N. Hoshino, T. Akutagawa, Y. Sado, R. Kitaura, H. Shinohara, K. Sugimoto, R. Zhang and Y. Murata, *Chem. Commun.*, 2014, **50**, 524–526.
6 S. A. FitzGerald, T. Yildirim, L. J. Santodonato, D. A. Neumann, J. R. D. Copley, J. J. Rush and F. Trouw, *Phys. Rev. B*, 1999, **60**, 6439–6451.
7 J. R. D. Copley, D. A. Neumann, R. L. Cappelletti and W. A. Kamitakahara, *J. Phys. Chem. Solids*, 1992, **53**, 1353–1371.
8 M. S. Dresselhaus, G. Dresselhaus and P. C. Eklund, *Science of Fullerenes and Carbon Nanotubes*, Academic Press, San Diego, 1996.
9 J. L. Dunn and C. A. Bates, *Phys. Rev. B*, 1995, **52**, 5996–6005.
10 P. R. Bunker and P. Jensen, *Fundamentals of Molecular Symmetry*, IOP Publishing, Bristol, 2005.
11 C. Beduz, M. Carravetta, J. Y.-C. Chen, M. Concistrè, M. Denning, M. Frunzi, A. J. Horsewill, O. G. Johannessen, R. Lawler, X. Lei, M. H. Levitt, Y. Li, S. Mamone, Y. Murata, U. Nagel, T. Nishida, J. Ollivier, S. Rols, T. Rõõm, R. Sarkar, N. J. Turro and Y. Yang, *Proc. Natl. Acad. Sci.*, 2012, **109**, 12894–12898.
12 K. S. K. Goh, M. Jimenez-Ruiz, M. R. Johnson, S. Rols, J. Ollivier, M. S. Denning, S. Mamone, M. H. Levitt, X. Lei, Y. Li, N. J. Turro, Y. Murata and A. J. Horsewill, *Phys. Chem. Chem. Phys.*, 2014, **16**, 21330–21339.
13 P. M. Felker, V. Vlček, I. Hietanen, S. FitzGerald, D. Neuhauser and Z. Bačić, *Phys. Chem. Chem. Phys.*, 2017, **19**, 31274–31283.
14 Z. Bačić, V. Vlcek, D. Neuhauser and P. M. Felker, *Faraday Discuss.*, 2018, doi:10.1039/C8FD00082D.
15 Y. Kohama, T. Rachi, J. Jing, Z. F. Li, J. Tang, R. Kumashiro, S. Izumisawa, H. Kawaji, T. Atake, H. Sawa, Y. Murata, K. Komatsu and K. Tanigaki, *Phys. Rev. Lett.*, 2009, **103**, 073001.
16 J. L. Dunn and E. Rashed, *J. Phys.: Conf. Ser.*, 2018, **1148**, 012003.
17 P. M. Felker and Z. Bačić, *J. Chem. Phys.*, 2016, **144**, 201101.
18 B. Poirier, *J. Chem. Phys.*, 2015, **143**, 101104.
19 B. Bransden and C. Joachain, *Introduction to Quantum Mechanics*, Longman Scientific and Technical, Harlow, England, 1989.
20 G. W. King, R. M. Hainer and P. C. Cross, *J. Chem. Phys.*, 1943, **11**, 27–42.
21 G. Herzberg, *Molecular Spectra & Molecular Structure III (Polyatomic Molecules)*, Van Nostrand, New Jersey, 1966.
22 A. G. Császár, G. Czakó, T. Furtenbacher, J. Tennyson, V. Szalay, S. V. Shirin, N. F. Zobov and O. L. Polyansky, *J. Chem. Phys.*, 2005, **122**, 214305.
23 M. Ge, U. Nagel, D. Huvonen, T. Room, S. Mamone, M. H. Levitt, M. Carravetta, Y. Murata, K. Komatsu, J. Y. C. Chen and N. J. Turro, *J. Chem. Phys.*, 2011, **134**, 13.
24 G. A. Dolgonos and G. H. Peslherbe, *Phys. Chem. Chem. Phys.*, 2014, **16**, 26294–26305.
25 A. Krachmalnicoff, R. Bounds, S. Mamone, S. Alom, M. Concistre, B. Meier, K. Kouril, M. E. Light, M. R. Johnson, S. Rols, A. J. Horsewill, A. Shugai, U. Nagel, T. Room, M. Carravetta, M. H. Levitt and R. J. Whitby, *Nat. Chem.*, 2016, **8**, 953–957.
26 A. B. Farimani, Y. Wu and N. R. Aluru, *Phys. Chem. Chem. Phys.*, 2013, **15**, 17993–18000.
27 M. Rigby, *The Forces between molecules*, Clarendon Press, Oxford, 1986.
28 P. M. Felker and Z. Bačić, *J. Chem. Phys.*, 2017, **146**, 084303.
29 S. Flügge, *Practical Quantum Mechanics*, Springer-Verlag, Berlin, 1974.
30 C. J. Bradley and A. P. Cracknell, *The Mathematical Theory of Symmetry in Solids*, Oxford University Press Inc, New York, 1972.
31 L. D. Hallam, C. A. Bates and J. L. Dunn, *J. Phys.: Condens. Matter*, 1992, **4**, 6775–6796.

32 Q. C. Qiu, *PhD thesis*, University of Nottingham, UK, 1998.

33 I. D. Hands, J. L. Dunn and C. A. Bates, *Phys. Rev. B*, 2010, **82**, 155425.

34 C. Robertson and G. A. Worth, *Chem. Phys.*, 2015, **460**, 125–134.

35 T. Zeng, R. J. Hickman, A. Kadri and I. Seidu, *J. Chem. Theory Comput.*, 2017, **13**, 5004–5018.

36 S. Mamone, M. Ge, D. Hüvonen, U. Nagel, A. Danquigny, F. Cuda, M. C. Grossel, Y. Murata, K. Komatsu, M. H. Levitt, T. Rõõm and M. Carravetta, *J. Chem. Phys.*, 2009, **130**, 081103.

37 K. S. K. Goh, *PhD thesis*, University of Nottingham, UK, 2015.

38 A. J. Horsewill, 2017, Private communication.

39 T. C. D. Group, *CP2K ver 2.4.0*, https://www.cp2k.org/, 2013.

40 S. Goedecker, M. Teter and J. Hutter, *Phys. Rev. B*, 1996, **54**, 1703–1710.

41 J. VandeVondele and J. Hutter, *J. Chem. Phys.*, 2007, **127**, 114105.

42 S. Grimme, J. Antony, S. Ehrlich and H. Krieg, *J. Chem. Phys.*, 2010, **132**, 154104.

43 C. N. Ramachandran and N. Sathyamurthy, *Chem. Phys. Lett.*, 2005, **410**, 348–351.

44 H. C. Longuet-Higgins, *Mol. Phys.*, 1963, **6**, 445–460.

45 D. J. Wales, *J. Chem. Phys.*, 1999, **110**, 10403–10409.

46 D. J. Wales, *J. Chem. Phys.*, 1999, **111**, 8429–8437.

47 D. J. Wales, *Recent Theoretical and Experimental Advances in Hydrogen Bonded Clusters*, Kluwer Academic Publishers, 2000, pp. 201–215.

48 A. Ceulemans and P. W. Fowler, *J. Chem. Phys.*, 1990, **93**, 1221–1234.

49 M. C. M. O'Brien, *Phys. Rev. B*, 1996, **53**, 3775–3789.

50 C. C. Chancey and M. C. M. O'Brien, *The Jahn-Teller effect in C_{60} and other icosahedral complexes*, Princeton University Press, Princeton, 1997.

51 H. Ramanantoanina, M. Gruden-Pavlovic, M. Zlatar and C. Daul, *Int. J. Quantum Chem.*, 2012, **113**, 802–807.

52 H. Ramanantoanina, M. Zlatar, P. Garcia-Fernandez, C. Daul and M. Gruden-Pavlovic, *Phys. Chem. Chem. Phys.*, 2013, **15**, 1252–1259.

53 H. S. Alqannas, A. J. Lakin, J. A. Farrow and J. L. Dunn, *Phys. Rev. B*, 2013, **88**, 165430.

54 I. D. Hands, J. L. Dunn and C. A. Bates, *Phys. Rev. B*, 2006, **73**, 235425.

55 O. Oliveira and A. Gonçalves, *Computational Chemistry*, 2014, **2**, 51–58.

56 M. D. Kaplan and B. G. Vekhter, *Cooperative phenomena in Jahn-Teller crystals*, Plenum Press, New York, 1995.

57 J. L. Dunn, *Phys. Rev. B*, 2004, **69**, 064303.

58 E. A. Moujaes and J. L. Dunn, *J. Phys.: Condens. Matter*, 2010, **22**, 085007.

59 A. L. Sobolewski, *Chem. Phys. Lett.*, 1997, **267**, 452–459.

60 L. Forró and L. Mihály, *Rep. Prog. Phys.*, 2001, **64**, 649.

61 J. L. Dunn and H. M. Li, *Phys. Rev. B*, 2005, **71**, 115411.

62 G. Klupp, K. Kamarás, N. M. Nemes, B. C. M. and J. Leão, *Phys. Rev. B*, 2006, **73**, 085415.

63 G. Klupp, P. Matus, K. Kamarás, A. Y. Ganin, A. McLennan, M. J. Rosseinsky, Y. Takabayashi, M. T. McDonald and K. Prassides, *Nat. Commun.*, 2012, **3**, 912.

64 N. Iwahara and L. F. Chibotaru, *Phys. Rev. Lett.*, 2013, **111**, 056401.

65 N. Iwahara and L. F. Chibotaru, *Phys. Rev. B*, 2015, **91**, 035109.